CHAMP Accelerometer Calibration by Means of the Equation of Motion and an a-priori Gravity Model

Christian Gruber, Dimitrios Tsoulis and Nico Sneeuw

Summary

Based on a one month CHAMP data set, accelerometer calibration parameters as well as harmonic coefficients of the geopotential at satellite altitude are estimated. The energy conservation principle is applied, with special regard to the observed non-gravitational forces. An orbital forces balance method leads to a bias parameter estimation for each axis of the **star** accelerometer. For validation purposes gravity fields have been calculated up to degree and order 60 with EIGEN2, GRIM5s1 and EGM96 models, which were used for the calibration of the accelerometer, revealing an agreement in geoid heights at dm-level.

Zusammenfassung

Basierend auf einem einmonatigen CHAMP-Datensatz werden Kalibrierungsparameter für das Akzelerometer sowie Geopotentialkoeffizienten auf Satellitenhöhe bestimmt. Dabei kommt das Energieerhaltungsprinzip zur Anwendung, unter besonderer Berücksichtigung der beobachteten nicht gravitativen Kräfte. Die resultierende Kräftebilanzmethode führt zu bias*-Schätzwerten für jede der drei Akzelerometer Achsen. Die zur Validierung berechneten Gravitationsfelder bis zu Grad und Ordnung 60, mit EIGEN2, GRIM5s1 und EGM96, die zur Kalibrierung des Akzelerometers benutzt wurden, zeigen eine Übereinstimmung bei den Geoidhöhen im Dezimeterbereich.*

1 Introduction

The non-conservative accelerations detected by CHAMP are of special interest for geopotential determination. They are required to convert the satellite's accelerations into gravitational forces. From high-low satellite to satellite tracking (hl-**sst**) observations the kinetic properties of CHAMP can be obtained and the Hamilton equation can be used to determine the potential energy. Due to mainly frictional forces of the Low Earth Orbiter (LEO) in the upper atmosphere, energy is withdrawn from the system and has therefore to be modeled in order to recover the potential. Due to the properties of accelerometers only a specific spectral bandwidth of the data can be used and a strategy has to be developed to calibrate the instrument in orbit. Proposed methods are satellite cross-over constraints (Gerlach et al. 2003) and in situ potentials from a known geopotential field (Han et al. 2003) that have been used to calibrate the along-track component as the main direction of drag forces during the movement through residual atmosphere in the upper ionosphere.

In the following approach all three axes of the accelerometer shall be calibrated in orbit from the balance of forces that can be obtained from an existing geopotential model such as EIGEN2 (Reigber et. al. 2003), GRIM5s1 (Biancale et. al. 2000) or EGM96 (Lemoine et. al. 1998) and the knowledge about the motion of the satellite. The resulting dissipative integrals are used to obtain a quasi independent geopotential solution and are compared to the respective geopotential model that was applied as a reference solution for the calibration.

The proposed method is based on calculating artificially the dissipative forces acting on CHAMP, as differences between the satellite's equation of motion, which associates the known orbital elements to final accelerations, and the sum of all gravitational forces acting on the satellite. Although the non-stationary gravity field is much more complicated in reality, we will only consider third-body forces due to Moon and Sun.

By comparing the computed dissipative forces with the available accelerometer data in a common reference frame, one can estimate calibration parameters and evaluate the respective dissipative integral. The accelerometer calibration will turn out to be mostly independent of the a priori gravity field so that the dissipative energy loss can be inferred consistently.

2 CHAMP configuration and related reference frames

The measurements on board of CHAMP are carried out by a GPS dual frequency, 16-channel receiver unit for precise orbit determination and a 3-axis STAR accelerometer with $3 \cdot 10^{-9}$ m s^{-2} precision in the along-track or cross-track directions and $3 \cdot 10^{-8}$ m s^{-2} precision in the radial direction, for the detection of non-conservative forces. To maintain the inclination and boom direction of the spacecraft, the attitude angles are determined by two Advanced Stellar Compass instruments and orbit corrections are carried out by thrusters.

The highly precise attitude determinations are based on pictures, taken by specialy designed electronic cameras.

Several reference frames are commonly used in CHAMP data processing. For an overview refer to (Schwintzer et al. 2002). Of special interest to this work is the spacecraft frame (SCF), the accelerometer instrument fixed frame (IFX) and the orbital or Gaussian frame. While a definition for the first two can be found in (Schwintzer et al. 2002), the Gaussian frame $\mathbf{e}_g = [\mathbf{s} \ \mathbf{t} \ \mathbf{n}]^\top$ has its origin at the center of mass of the satellite, $\mathbf{s}$ stands for the radial component of the Gaussian basis (radius vector from orbital center, lying in the orbital plane), $\mathbf{n}$ is

the cross-track component and **t** denotes the quasi along-track component (completing the triad). It should be mentioned that this frame is radially earth pointing thus deviating from the local orbital frame by the orbit eccentricity.

CHAMP has been launched into an almost circular, near polar orbit with 87 degrees of inclination against the equatorial plane and a mean altitude of initially 454 km that has already declined to 408 km at the point where the data for the present study were acquired, namely $01.07.02 - 30.07.02$. The satellite is losing about 43 m per day in height during this period and the revolution duration is about 93 min, which corresponds to a linear speed of approximately 7.5 kms^{-1} over ground.

The measurement bandwidth (MWB) of the accelerometer device is specified within 10^{-1}Hz $- 10^{-4}$Hz. This implies, that non-gravitational effects caused by processes lasting shorter then 10 s or longer than 2 subsequent revolutions (up to constant offsets) are outside the MWB and have to be taken care of by a calibration principle in order to extract the dissipative information. Finally, the sampling rate of the available GPS-based positions given in the international terrestrial reference frame ITRF is 1/30 Hz and that of both the accelerometer and the attitude angles in the instrument fixed frame 1/10 Hz.

3 Methodology

The calibration of the accelerometer is an essential step in gravity field determination from CHAMP. Apart from some a-priori estimates of the accuracy (or sensitivity) of the device, there exists hardly an accurate and reliable method for the independent estimation of its bias and scale, using the available observed accelerometer data. However, although their exact mathematical description is not feasible, one may compute indirectly the value of non-gravitational accelerations along the orbit, at the identical points where the accelerometer data have been obtained. This permits the direct comparison of these theoretically evaluated non-gravitational accelerations with those registered by the STAR device, which leads to a calibration parameter estimation for the accelerometer.

The motion of a satellite orbiting the Earth is the combined result of gravitational and non-gravitational forces acting on it, the latter being measured by the CHAMP accelerometer. With the gravitational part coming mainly from Earth, Sun and Moon, one may generally write

$$\overline{\mathbf{F}} = \frac{d}{dt}\mathbf{v} - \nabla V, \tag{1}$$

where $d\mathbf{v}/dt$ denotes the total acceleration acting on the satellite with **v** its velocity vector, $\overline{\mathbf{F}}$ stands for the non-gravitational forces, the gravitational part due to the Earth and other third body potentials (here only Sun and Moon are considered) is given by ∇V. Both $\overline{\mathbf{F}}$ and ∇V

describe forces per unit mass, having thus the same dimensions as $d\mathbf{v}/dt$. Comparing the measured accelerations from CHAMP with some generated ones by (1) gives theoretically the ability to calibrate the instrument.

Kinematics

Before building the linear model for the calibration of the accelerometer, let us first comment on the numerical evaluation of the terms on the right hand side of Equation (1). Given the position of the satellite in terms of its radius vector **r** and its velocity **v** one may proceed to the numerical computation of $d\mathbf{v}/dt$ in the Gaussian frame employing the so called Hill variables (Cui 1997),

$$\frac{d}{dt}\mathbf{v} = \left(\frac{d\dot{r}}{dt} - \frac{G^2}{r^3}\right)\mathbf{s} + \frac{1}{r}\frac{dG}{dt}\mathbf{t}$$
$$+ \frac{G}{r}\left(\cos u \frac{di}{dt} + \sin u \sin i \frac{d\Omega}{dt}\right)\mathbf{n}, \tag{2}$$

where $\dot{r}$ denotes the radial derivative of the radius vector (radial velocity), G the magnitude of the angular momentum vector, u, i, Ω are the argument of latitude, the orbit inclination and the right ascension of the ascending node respectively. The computation of the Hill variables G, $\dot{r}$, u, and Ω entering the right hand side of equation (1) has been carried out in the frame of this work by means of closed expressions involving **r** and **v** provided by Rapid Science Orbits from the CHAMP Information System and Data Center (ISDC) at Geoforschungszentrum (GFZ) Potsdam. The subsequent time derivatives have been obtained component wise by a numerical differentiation scheme based on central differences and a Taylor series expansion in the center point, leading to an equation system for the derivatives that can be solved e.g. in the case of three central differences for the first derivative as (cf. Mai 1997)

$$f' = \frac{1}{10}(15\Delta^1 - 6\Delta^2 + \Delta^3), \tag{3}$$

where the Δ^j are the centered differences between equidistant data points,

$$\Delta^j = \frac{y_{k+j} - y_{k-j}}{2j}. \tag{4}$$

The solution is equivalent to what is often refered to as Newton-Gregory differentiation and can be found in numerous textbooks on numerical differentiation.

Dynamics

The second term that has to be computed for the synthesis of the dissipative forces acting on the CHAMP satellite according to Equation (1), is the gravitational part ∇V. Denoting with $V_{\oplus}$ and V_{3rd} the gravitational potential due to Earth and other third bodies (Sun and Moon) respectively, one can write $\nabla V = \nabla V_{\oplus} + \nabla V_{3rd}$. For the evaluation of $V_{\oplus}$ a spherical harmonic series expansion may be applied, using one of the available Earth gravity models. In this way a reference model is introduced for

the calibration of the CHAMP accelerometer. $V_\oplus$ can be obtained by the standard expression

$$V_\oplus = \frac{\mu}{r} + \frac{\mu}{r} \sum_{n=2}^{N} \sum_{m=0}^{n} \left(\frac{a_e}{r}\right)^n \overline{P}_{nm}(\cos\theta)$$
$$(\overline{c}_{nm} \cos m\lambda + \overline{s}_{nm} \sin m\lambda) \ , \qquad (5)$$

a_e denotes a semi major axis of an Earth ellipsoid, r, λ, θ are spherical (geocentric) coordinates of the computation point, μ stands for the universal gravitational constant times a mean Earth mass, $\overline{P}_{nm}$ are the normalized associated Legendre functions of degree n and order m and $\overline{c}_{nm}, \overline{s}_{nm}$ are the normalized spherical harmonic coefficients of the given Earth gravity model, available up to the respective maximum degree and order N.

Differentiation of $V_\oplus$ with respect to θ, λ and r leads to the gradient of the geopotential in the local tangent frame:

$$\nabla V_\oplus = \begin{pmatrix} f_r \\ f_\theta \\ f_\lambda \end{pmatrix} = \begin{pmatrix} \partial V/\partial r \\ 1/r \cdot \partial V/\partial\theta \\ 1/r\sin\theta \cdot \partial V/\partial\lambda \end{pmatrix} . \qquad (6)$$

The force components read finally

$$f_r = \sum_{n=0}^{N} \sum_{m=0}^{n} -(n+1)\frac{\mu}{r^2}\left(\frac{a_e}{r}\right)^n \overline{P}_{nm}(\cos\theta)$$
$$(\overline{c}_{nm}\cos m\lambda + \overline{s}_{nm}\sin m\lambda) \ ,$$

$$f_\theta = \frac{\mu}{r^2} \sum_{n=2}^{N} \sum_{m=0}^{n} \left(\frac{a_e}{r}\right)^n \frac{d}{d\theta}\overline{P}_{nm}(\cos\theta)$$
$$(\overline{c}_{nm}\cos m\lambda + \overline{s}_{nm}\sin m\lambda) \ ,$$

$$f_\lambda = \frac{\mu}{r^2} \sum_{n=2}^{N} \sum_{m=0}^{n} \left(\frac{a_e}{r}\right)^n \frac{1}{\sin\theta}\overline{P}_{nm}(\cos\theta)$$
$$(\overline{s}_{nm}\cos m\lambda - \overline{c}_{nm}\sin m\lambda) \ . \qquad (7)$$

In the sequel, the cartesian counterparts of these force components in the Earth fixed frame ITRF will be of interest. Thus, the following expressions are computed

$$\nabla V_\oplus = \begin{pmatrix} f_x \\ f_y \\ f_z \end{pmatrix}$$
$$= \begin{pmatrix} f_r\sin\theta\cos\lambda + f_\theta\cos\theta\cos\lambda - f_\lambda\sin\lambda \\ f_r\sin\theta\sin\lambda + f_\theta\cos\theta\sin\lambda + f_\lambda\cos\lambda \\ f_r\cos\theta - f_\theta\sin\theta \end{pmatrix} . \qquad (8)$$

4 Definition of a calibration model for the accelerometer

In order to compare the dissipative forces as computed by equation (1) with the accelerometer data of CHAMP, both have to refer to a common reference frame. Up to now the computation of the dissipative forces according to (1) has been presented for the orbital (Gaussian) reference frame. The accelerometer data of CHAMP refer, on

the other hand, to an instrument fixed frame (IFX). The alignment between instrument fixed and orbital frame can be calculated as a single rotation about one rotational axis by means of quaternion algebra, cf. (Grewal et al. 1997). By means of attitude quaternions, provided by the Star Tracking device and the relations to the orbital frame, the dissipative forces (1) can be transformed from the orbital frame into the instrument fixed frame of the three accelerometer axes. The resulting transformation takes finally the form of small misalignment angles and has been found to oscillate about $\pm 2°$ about the orbital reference system, depending on the actual position of the spacecraft, since the boom direction automatically orientates into the direction of the strongest drag.

Having transformed by means of quaternion algebra $\overline{\mathbf{F}}$ to $\overline{\mathbf{F}}_{IFX}$, a calibration system may be set up, comparing the computed dissipative accelerations obtained by (1) to the observables registered by the accelerometer according to

$$\overline{\mathbf{F}}_{IFX} + \boldsymbol{\epsilon}_F = \mathbf{B} + (\mathbf{A}_{IFX} + \boldsymbol{\epsilon}_A), \qquad (9)$$

where $\overline{\mathbf{F}}_{IFX}$ are the non-gravitational forces expressed in the instrument fixed frame, $\mathbf{A}_{IFX}$ the accelerometer measurements, where the original accelerometer sampling rate of 10 s has been decimated to the rate of 30 s in order to coincide with the computed $\overline{\mathbf{F}}_{IFX}$, $\boldsymbol{\epsilon}_F$ and $\boldsymbol{\epsilon}_A$ give the error of $\overline{\mathbf{F}}_{IFX}$ and $\mathbf{A}_{IFX}$ respectively and finally $\mathbf{B}$ denotes the unknown instrument bias as a function of time.

Although $\boldsymbol{\epsilon}_A$ has a very small value, according to the instrument's specifications, $\boldsymbol{\epsilon}_F$ obtains very large values, obviously due to the use of GFZ's rapid science orbit information and the derivation step. The error magnitudes of $\boldsymbol{\epsilon}_F$ exceed the required precision for the bias estimates up to 2 orders of magnitude. Application of a properly defined smoothing operator to $\overline{\mathbf{F}}_{IFX}$ would therefore decrease $\boldsymbol{\epsilon}_F$ considerably and allows a direct bias estimation from equation (9). It should be noted here, that the GFZ provided correction terms for the radial component as well as the scale parameters in each axis have been applied, so that no benefit from the introduction of an additional scale parameter could be found. Furthermore, in order to properly estimate scale and bias parameters simultaneously from short data windows a-priori covariance information would be required to separate cross-correlation.

With the bias approach being followed here no physical assumptions about the instrument behaviour have been made yet. By filtering the bias with respect to the accelerometer MWB compliance to the instrument specifications shall be achieved, leaving possible unconsidered systematic effects in the calibrated data.

It can be expected that frequencies in the range of $1 \cdot 10^{-4}$ Hz $- 1 \cdot 10^{-1}$ Hz will be represented by the measured time series. In the time domain this corresponds to wavelengths with a period of 10 s up to roughly 2 revolutions (185 min). A dirac-like sequence has been used in order to construct an approximating function for both,

the computed dissipative forces and the accelerometer data leaving a bias with expectable smooth characteristics. The hereby used kernel function follows the theory of delta functions, and is given by (Shilov 1973):

$$f_n(y) = \int_0^1 C_n \left[1 - (x - y)^2\right]^n f(x)\, dx, \qquad (10)$$

with

$$C_n = \frac{1}{\int_{-1}^1 (1 - t^2)^n dt}, \qquad (11)$$

being a scale factor.

A trial function $f(y)$ will be approximated by means of this smoothing kernel in terms of a sequence of polynomials of degree $\leq 2n$ defining the particular correlation length. The kernel (10) has been applied to $\overline{\mathbf{F}}_{\mathrm{IFX}}$ using a correlation length of 30 epochs. Due to its spectral characteristics this definition of n leds to a considerable damping of ϵ_F in the higher frequency band, while its application to the computed dissipative forces produces time series that are in the medium band comparable to those obtained from CHAMP's accelerometry. Fig. 1 displays a section of the along-track component of $\mathbf{A}_{\mathrm{IFX}}$ as provided by the raw measurements and the same component of $\overline{\mathbf{F}}_{\mathrm{IFX}}$ as computed by (1) and smoothed by (10) for the one month CHAMP data used (July 2002). The two signals correlate smoothly through the given period of data producing differences of the order of $10^{-8}\,\mathrm{ms}^{-2}$.

After the application of kernel (10) to the computed $\overline{\mathbf{F}}_{\mathrm{IFX}}$ a direct bias estimation for all three axes of the accelerometer device can be carried out from equation (9). Fig. 2 presents the bias estimation for along-track, cross-track and radial component of the accelerometer for the given thirty days period. The biases have been obtained by simply comparing component-wise the smoothed $\overline{\mathbf{F}}_{\mathrm{IFX}}$ with the measurements $\mathbf{A}_{\mathrm{IFX}}$. The resulting bias estimates have been furthermore averaged over 2 revolutions and are plotted over the entire sequence of one month in Fig. 2. The bias estimates reveal in overall a rather stable course with relatively smooth fluctuations over some constant values ($-2.96 \cdot 10^{-6}\,\mathrm{ms}^{-2}$, $-2.7 \cdot 10^{-7}\,\mathrm{ms}^{-2}$ and $8.425 \cdot 10^{-5}\,\mathrm{ms}^{-2}$ for the along-track, cross-track and radial component respectively).

Having estimated the bias parameters for all three accelerometer axes we may now compute the respective energy loss $\int \mathbf{A}_{\mathrm{IFX}}\, \mathbf{v}\, dt$ resulting from each accelerometer axis taking also the bias information into account[1]. Fig. 3 shows this energy loss for each component after accelerometer calibration. The dominance of the along-track component is evident as well as expected. Interesting however is the contribution of the other two components to the total energy loss, depicted in the respective subplots of Fig. 3. Although representing a very small fraction with respect to the effect of the along-track component, their contribution should be certainly taken into account, especially when longer data sequences are analyzed.
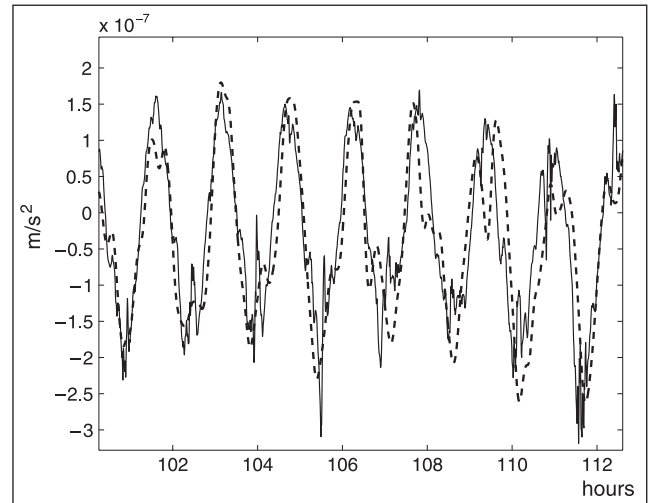

Fig. 1: Along-track accelerometer signal (continuous line) compared to its computed along-track component (dashed line) generated by (1) and approximated by (10) for CHAMP data (time since July 1th, 2002).
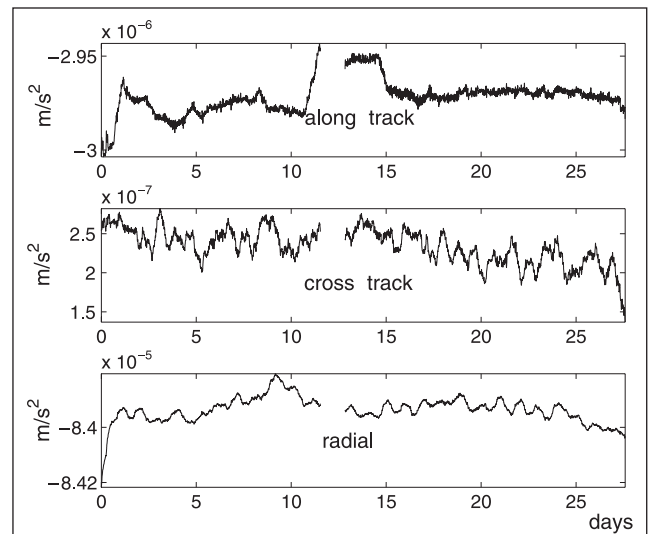

Fig. 2: Bias estimates, calculated as average over 2 revolutions for the 3-axis accelerometer over a 30 day period (July 2002), estimated separately for the along-track, cross-track and radial component. The gap at day 12 is due lack of accelerometer data.

5 The Hamilton Equation

In order to evaluate some computed accelerometer calibration parameters the calculation of spherical harmonics shall be processed by the energy balance equation. The energy of the CHAMP satellite is generally assumed to be a constant of motion. With V the total gravitational potential and T denoting the sum of kinetic and centrifugal potentials the Hamilton equation should hold

---

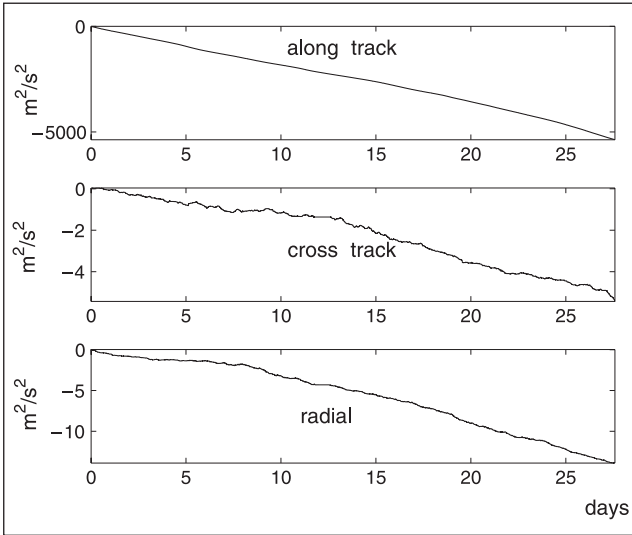1 The gap has been filled by the dissipative forces derived from the orbital data.

Fig. 3: Energy dissipation given in instrument fixed frame: along–track, cross–track and radial component

$$H = T + V \tag{12}$$

with H being a constant. When introducing non-conservative forces $\overline{\mathbf{F}}$ along the orbit in the Earth fixed reference frame (measured by accelerometry for the CHAMP experiment), H is not constant in time and the above equation can be rearranged to (compare Gerlach et al. 2003)

$$V_{\oplus} + V_{3rd} + H = \frac{1}{2}\mathbf{v}_{\text{ef}} \cdot \mathbf{v}_{\text{ef}} - \frac{1}{2}(\boldsymbol{\omega} \times \mathbf{r}_{\text{ef}}) \cdot (\boldsymbol{\omega} \times \mathbf{r}_{\text{ef}}) \\ - \int_{t_o}^{t} \overline{\mathbf{F}} \cdot \mathbf{v}_{\text{ef}} \, dt, \tag{13}$$

where the subscript 'ef' refers to the Earth fixed frame ITRF and $\boldsymbol{\omega}$ represents the vector of the Earth's rotation $[0 \ 0 \ d\Theta/dt]$, Θ being the Greenwich Apparent Sidereal Time. The integration of the dissipative forces along the orbit in the Earth fixed reference frame should hold due to the rotation of the atmosphere (in the case of a LEO). Expressing the velocities in a quasi-interial non rotating equatorial frame

$$\mathbf{v} = \mathbf{R}^{\top}(\mathbf{v}_{\text{ef}} + \boldsymbol{\omega} \times \mathbf{r}_{\text{ef}}), \tag{14}$$

where R denotes the transformation from space fixed to Earth fixed coordinates and includes information about the instantaneous parameters of the polar motion and of Θ (for definitions see e.g. Montenbruck and Gill 2000), equation (13) can be reformulated in this quasi-intertial frame:

$$V_{\oplus} + H = \frac{1}{2}\mathbf{v} \cdot \mathbf{v} + \boldsymbol{\omega} \cdot (\mathbf{v} \times \mathbf{r}) \\ - \int_{t_o}^{t} (\overline{\mathbf{F}} + \nabla V_{3rd}) \cdot (\mathbf{v} + \boldsymbol{\omega} \times \mathbf{r}) \, dt, \tag{15}$$

as the energy balance equation, that can be directly adopted for the orbital frame using equation (1). A more rigorous approach for the derivation of the Hamiltonian

can be found in Jekeli (1999), assuming the rotational term with $(\boldsymbol{\omega} \times \mathbf{r})$ as being of negligible small amplitude. The third body potential has now been treated as a force integral on the right hand side of (15) in order to maintain complementarity to the surface forces, that have been determined from (1).

6 Gravity field recovery

After the accelerometer calibration has been completed, one may obtain a time series of the Earth's gravitational potential along the orbit using equation (15), by replacing $\overline{\mathbf{F}}$ in the last term of its right hand side with simply $\mathbf{A}_{\text{IFX}}$, $\mathbf{A}_{\text{IFX}}$ denoting the calibrated accelerometer data. Radial continuation of these values onto a sphere at mean satellite altitude with a Taylor series expansion along the radial direction, followed by an interpolation of this orbit correlated potential distribution by means of a standard 2-dimensional gridding function, we obtain a formal raster of potential values on a sphere at satellite altitude. From this point it is straightforward to perform spherical harmonic analysis in order to derive the set of spherical harmonic coefficients that corresponds to the given potential data on the sphere (see e.g. Tsoulis 1999).

Using the **Matlab** bundle `gsha` (Tsoulis and Sneeuw 1998) a set of potential harmonic coefficients from the given potential values is computed in a least squares adjustment, where the full system of normal equations was solved with no regularization applied. Spectral downward continuation to zero level then leads to a global gravity model that is complete up to degree and order 60 and its signal degree variance with model EIGEN2 used as the reference model entering equations (6) is presented in Fig. 4 with the dashed line. In the same Figure depicted are the power spectrum of Kaula's rule (solid line), the spectrum of the difference between EGM96 and EIGEN2 models (thick line) and the spectra of differences between EIGEN2 and our calibration solution (three thin lines) using three different reference models, namely GRIM5s1, EIGEN2 and EGM96 according to

$$\sigma_l = \sqrt{\sum_{m=0}^{l} [(\overline{c}_{lm}^{(EIGEN2)} - \overline{c}_{lm})^2 + (\overline{s}_{lm}^{(EIGEN2)} - \overline{s}_{lm})^2]}, \tag{16}$$

with $\overline{c}_{lm}$ and $\overline{s}_{lm}$ the harmonic coefficients emerging from the different calibration solutions. It is also important to mention that all degree variances are computed for degrees $l \geq 2$. It becomes evident from Fig. 4 that no matter which reference gravity model is used the coefficients computed by the current method seem to be of very good agreement with those of model EIGEN2, at least up to degree 40. At higher frequencies this correspondence is less evident but this could be due to the short data of one month only and the coefficient estimation method be-
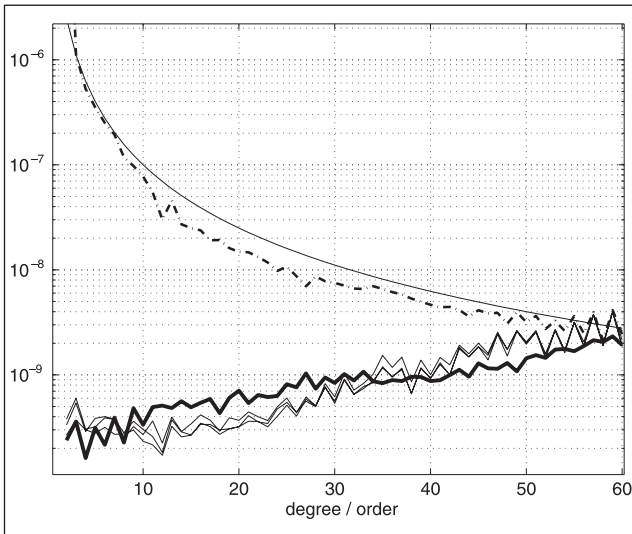
Fig. 4: Spectral power of geopotential coefficients per degree. Solid line: Kaula's rule, dashed line: solution calibrated with EIGEN2, thin lines: solutions calibrated with different Earth models (GRIM5s1, EIGEN2 and EGM96) plotted as differences to EIGEN2, thick line: EGM96 minus EIGEN2.
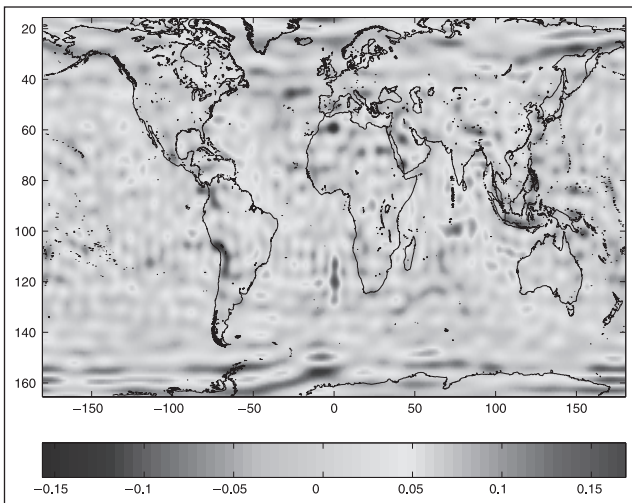

Fig. 5: Solution calibrated with EIGEN2 plotted as difference to EIGEN2 in geoid heights in [m] at orbit level (±15° latitude bands around the poles are excluded).

ing applied. In overall the result is in good accordance to the fact that EIGEN2 includes the STAR accelerometry data. Fig. 5 shows the differences to the reference model in terms of geoid heights after a synthesis step with the computed model coefficients.

To obtain a first measure of the quality of the newly computed geopotential coefficients a forward computation of global geoid heights at satellite level by means of a direct spherical harmonic synthesis step up to degree and order 60 has been carried out and compared to the respective models that have been used for the calibration. Tab. 1 lists the standard deviations of the differences in geoid height at orbit level for co-latitudes 11° to 170°.

Two facts become evident from these comparisons. On the one hand, the computed field strongly depends on the reference gravity field used for the calibration. At the same time all three models agree very well with EIGEN2.

Tab. 1: Standard deviations of differences between global distributed geoid heights in [m] at satellite level calculated from the present solution for different calibration models minus geoid heights from different Earth gravity models (±10° latitudes around the poles are excluded).

Potential field used for calibration	Models that are used for comparison		
	EGM96	EIGEN2	GRIM5s1
EGM96	0.095	**0.087**	0.166
EIGEN2	0.099	**0.086**	0.165
GRIM5s1	0.100	**0.088**	0.162

7 Discussion

A further detailed investigation of the following central issues should provide an insight into the restrictions from the present approach as well as the quality of the obtained gravity model and at the same time give hints for solutions of increased resolution and accuracy:

- verification of the used input data, especially the orbit data and the differentiation step. Outlier detection methods should be applied to obtain more reliable accelerations from the orbital data. Since the noise ratio between accelerometer and double differentiated orbit positions is of about two orders of magnitude, enhancements concerning the reliablitity of the orbit shall thus directly improve the capability to calibrate the accelerometer.

- the gravity field recovery step to investigate the quality of the calibration. The parameter estimation should be carried out in situ, thereby avoiding field continuation as well as data interpolation onto a regular grid. Better spatial coverage and more redundancy should also enhance results.

- the applied filtering of the bias to decorrelate from the used reference field as well as to reduce the noise ratio could be investigated by simulative studies.

- convergent iteration, generating in each step calibrated accelerometry data as well as new gravity field parameters could possibly make the approach independent of external information.

8 Conclusions

An alternative method for the calibration of the CHAMP accelerometer is discussed, by comparing synthetically

derived dissipative forces based on the definition of the equation of motion with the accelerometry measurements of CHAMP. In order to obtain some more information on the quality of the calibration results that were obtained, a respective preliminary gravity model was evaluated as well and compared with some standard gravity models. The overall method is per definition strongly dependent on the accuracy of the used orbits. This leads to a first priority for future considerations, namely the application of more precise orbits (dynamic, reduced-dynamic or kinematic) and the assessment of their effect on the calibration parameter estimation, or even on the computed gravity fields. The particular feature of the present contribution, that is offering more insight on the calibration problem, by estimating parameters for all three accelerometer axes, should be, in our opinion, further exploited in CHAMP-related studies.

Acknowledgements

References

Biancale R., Balmino G., Lemoine J.-M., Marty J.-C., Moynot B., Barlier F., Exertier P., Laurain O., Gegout P., Schwintzer P., Reigber Ch., Bode A., Gruber Th., Knig R., Massmann F.-H., Raimondo J.C., Schmidt R., Zhu S.Y.: A new global Earth's gravity field model from satellite orbit perturbations: GRIM5-S1. Geophysical Research Letters, Vol. 27, No. 22, p. 3611–3614, 2000.

Cui C., Mareyen M.: Gauss's equations of motion in terms of Hill variables and first application to numerical integration of satellite orbits. manuscr geod 17: 155–163, 1992.

Cui C.: Satellite Orbit Integration based on Canonical Transformations with Special Regard to the Resonance and Coupling Effects. Deutsche Geodätische Kommission, Reihe A, Heft Nr. 112, München 1997.

Gerlach C., Sneeuw N., Visser P., Svehla D.: CHAMP Gravity Field Recovery with the Energy Balance Approach: First Results. In Reigber C., Lühr H., Schwintzer P. (Eds), First CHAMP Mission Results for Gravity, Magnetic and Atmospheric Studies, pp. 134–139, Springer, 2003.

Grewal M.S., Weill L.R., Andrews A.P.: Global Positioning Systems, Inertial Navigation, and Integration. John Wiley & Sons Inc., 2001.

Han S.C., Jekeli C., Shum C.K.: Efficient gravity gield recovery using in situ disturbing potential observables from CHAMP. Geophys Res Let 29 (16), 10.1029/2002GL015180, 2002.

Lemoine F.G., Kenyon S.C., Factor J.K., Trimmer R.G., Pavlis N.K., Chinn D.S., Cox C.M., Klosko S.M., Luthcke S.B., Torrence M.H., Wang Y.M., Williamson R.G., Pavlis E.C., Rapp R.H. and Olson T.R.: The Development of the Joint NASA GSFC and NIMA Geopotential Model EGM96, NASA/TP-1998-206861, NASA Goddard Space Flight Center, Greenbelt, Maryland, 20771 USA, July 1998.

Jekeli C.: The determination of gravitational potential differences from satellite-to-satellite tracking. Cel Mech Dyn Astron 75: 85–101, 1999.

Mai E.: Zum Dynamischen Inversionsproblem in der Satellitenbahntheorie, Diplomarbeit, TU Berlin, 1997.

Montenbruck P., Gill E.: Satellite Orbits. Springer Verlag, Berlin-Heidelberg, 2000.

Reigber Ch., Schwintzer P., Neumayer K.-H., Barthelmes F., Knig R., Förste Ch., Balmino G., Biancale R., Lemoine J.-M., Loyer S., Bruinsma S., Perosanz F., Fayard T.: The CHAMP-only Earth Gravity Field Model EIGEN-2. Advances in Space Research 31 (8), 1883–1888, 2003.

Schwintzer P., Lühr H., Reigber, C., Grunwaldt L., Förste Ch.: CHAMP Reference Systems, Transformations and Standards. GFZ Technical Note CH-GFZ-RS-002, GFZ Potsdam, 2002.

Shilov G.E.: Elementary Functional Analysis. MIT Press, Cambridge, Massachusetts, 1974.

Tsoulis D., Sneeuw N.: gsha: a MATLAB software for global spherical harmonic analysis. Technical University of Munich, Institute of Astronomical and Physical Geodesy, 1998.

Tsoulis D.: Spherical harmonic computations with topographic/isostatic coefficients. IAPG/FESG reports series, Rep No 3, Institute of Astronomical and Physical Geodesy, Technical University of Munich, 1999.

Authors' address

Dipl.-Ing. Christian Gruber
Institute of Navigation and Satellite Geodesy
Technical University of Graz
Steyrergasse 30/III, A-8010 Graz, Austria
Fax: +43 316 873-6845
gruber@geomatics.tu-graz.ac.at

Ass. Prof. Dr-Ing. Dimitrios Tsoulis
Department of Geodesy and Surveying
Aristotle University of Thessaloniki
Univ Box 440, 54124 Thessaloniki, Greece
Fax: +30 2310 995948
tsoulis@topo.auth.gr

Ass. Prof. Dr.-Ing. Nico Sneeuw
Department of Geomatics Engineering
University of Calgary
2500 University Drive, Calgary, Alberta, T2N 1N4, Canada
Fax: +1 403 284-1980
sneeuw@ucalgary.ca